PCCP

Cite this: *Phys. Chem. Chem. Phys.*, 2011, **13**, 17494–17504

www.rsc.org/pccp

PAPER

Recombination and chemical energy accommodation coefficients from chemical dynamics simulations: O/O_2 mixtures reacting over a β-cristobalite (001) surface

Víctor Morón,[a] Pablo Gamallo,[ac] Ludovic Martin-Gondre,[bc] Cédric Crespos,[d] Pascal Larregaray[d] and Ramón Sayós*[a]

Received 19th March 2011, Accepted 19th August 2011
DOI: 10.1039/c1cp20828d

A microkinetic model is developed to study the reactivity of an O/O_2 gas mixture over a β-cristobalite (001) surface. The thermal rate constants for the relevant elementary processes are either inferred from quasiclassical trajectory calculations or using some statistical approaches, resting on a recently developed interpolated multidimensional potential energy surface based on density functional theory. The kinetic model predicts a large molecular coverage at temperatures lower than 1000 K, in contrary to a large atomic coverage at higher temperatures. The computed atomic oxygen recombination coefficient, mainly involving atomic adsorption and Eley-Rideal recombination, is small and increases with temperature in the 700–1700 K range ($0.01 < \gamma_O < 0.02$) in good agreement with experiments. In the same temperature range, the estimated chemical energy accommodation coefficient, the main contribution to which is the atomic adsorption process is almost constant and differs from unity ($0.75 < \beta_O < 0.80$).

1. Introduction

The reentry of space vehicles into Earth's atmosphere, involves hypersonic speeds. The corresponding hypersonic flows are usually characterized by strong shocks leading to equilibrium or nonequilibrium molecular plasmas.[1,2] Elementary processes involving atomic/molecular oxygen and nitrogen in the boundary layer are catalysed by the materials used as thermal protection systems (TPS) of these vehicles, increasing the total heat flux to their surfaces. The seeming simple heterogeneous processes that happen in these extreme conditions (*e.g.*, O adsorption, O_2 dissociative adsorption, O recombination *via* an Eley–Rideal mechanism,...) are even nowadays difficult to study experimentally or theoretically.[3,4] Computer fluid dynamics (CFD) simulations are usually carried out to predict the relevant aerothermodynamics.[1] In these simulations two coefficients are required to include appropriately the wall catalycity effects: (a) the atomic recombination coefficient γ_i (also called catalytic efficiency),[3,4] which is the recombination probability of the i atomic species on the surface and (b) the chemical energy accommodation coefficient β_i,[3–5] defined as the ratio of energy released to the surface per atomic recombination to the maximum energy transferable. Both coefficients are within the range $0 \leq \gamma_i, \beta_i \leq 1$ (for air i will be essentially O and N) and are supposed to depend on temperature and total/partial pressures (*i.e.*, γ_i (T, P)) although more detailed description would be required for CFD accurate simulations of nonequilibrium flows (*e.g.*, γ_i (T_{gas}, $T_{surface}$, P)). Nevertheless, many experiments only measure routinely the effective catalycity ($\gamma_{eff,i} = \gamma_{i'} = \gamma_{i'}\beta_i$).

Experimental γ_i and β_i values are characterized by a broad scatter[4] since they depend on the conditions under they were measured. According to this, the use of these coefficients does not properly describe the heat transfer over the whole surface and the entire trajectory of the vehicle. The important effect of γ_i coefficient on the heat flux has been shown in several simulations;[3,6] some studies yield up to a factor of two for the wall heat flux of a fully catalytic wall (*i.e.*, $\gamma_i = 1$) wall compared to a noncatalytic one (*i.e.*, $\gamma_i = 0$). The β_i coefficient is hardly measured and often it is taken equal to 1 (*i.e.*, fully energy accommodation assumption), although available values are very far from one.[4] Therefore, more experimental or theoretical γ_i and β_i values would be necessary to better design thermal shields for spacecrafts, which would also allow a payload improvement.

Recombination and surface activity data for silica-based materials are important as those are commonly used in TPS (*e.g.*, in space shuttle tiles). Measurements of oxygen and

[a] *Departament de Química Física and Institut de Química Teòrica i Computacional, Univ. Barcelona, C. Martí i Franquès 1, 08028 Barcelona, Spain. E-mail: r.sayos@ub.edu*
[b] *Centro de Física de Materiales (CFM), Centro Mixto CSIC-UPV/EHU, P. Manuel de Lardizabal 5, 20018 San Sebastián, Spain*
[c] *Donostia International Physics Center (DIPC), P. Manuel de Lardizabal 4, 20018 San Sebastián, Spain*
[d] *Institut des Sciences Moleculaires, UMR 5255 CNRS-Université Bordeaux I, 33405 Talence Cedex, France*

nitrogen coefficients for air and O_2 or N_2 pure gases over SiO_2-based surfaces (*i.e.*, γ_i, $\gamma_{i'}$, β_i on quartz, cristobalite, RCG, vitreosil, pyrex, silicon carbide,...) have been recently reviewed.[4,7] γ_i coefficients show strong temperature dependence, increasing with temperature until a critical value where the thermal desorption becomes significant and hence the recombination coefficient declines. In particular, there are measurements of γ_O[8] and β_O[9] for air at 200 Pa over β-cristobalite at high temperatures (800–1830 K), which were obtained by *in situ* oxidation of sintered SiC samples.

A large number of kinetic models for dissociated air, O_2 and N_2 gases on silica like surfaces have been developed in the past.[6,10–17] These models take into account the main surface processes: physisorption, chemisorption, dissociative adsorption, thermal desorption, Eley–Rideal (ER) or Langmuir–Hinshelwood (LH) atomic recombinations. The microscopic parameters used in these models (*e.g.*, desorption energies, activation energies, density of adsorption sites, *etc*) may be either derived from quantum-mechanical calculations or from semiempirical formulas. However, such parameters usually are estimated by fitting the experimental $\gamma_i(T)$ coefficients or the heat fluxes.[3] Thus, $\gamma_i(T, P)$ curves are reported although different sets of kinetic parameters can predict the same heat flux. Apart from macroscopic one-temperature models, more advanced state-to-state models have also been used in the description of the nonequilibrium chemical kinetics of high temperature plasmas.[18] The state-to-state approach describes any internal degree of freedom of the molecules (vibrational, rotational, electronic). Each level is considered as an independent species subject to an appropriate continuity equation, own cross sections and rate coefficients. From the level distributions, the thermal properties of the gas and the global rate coefficients are derived, which may significant differ from those attained by a thermal equilibrium or weak nonequilibrium analysis. Thus, nonequilibrium vibrational kinetics of an O_2/O mixture[19] or air[20] hitting a catalytic silica surface has been investigated.

In a previous study of the O/SiO_2 system, we carried out Density Functional Theory (DFT) calculations of O adsorption over a β-cristobalite (001) surface, showing a strong chemisorption.[21] Quasiclassical trajectory studies (QCT) of atomic oxygen on a clean[22] or O-precovered[23,24] β-cristobalite (001) surface reveal the importance of the atomic adsorption or penetration into the SiO_2 slab (absorption) along with the formation of adsorbed ($O_{2(ad)}$) and gas phase ($O_{2(gas)}$) molecular oxygen; these latter species mainly were formed through an Eley-Rideal (ER) mechanism. The O_2 scattering on a clean β-cristobalite (001) surface[24,25] produces principally reflection and sticking (absorption/adsorption), while the dissociative sticking is only open at high collision energies (*i.e.*, $E_i > 1$ eV). Other authors have also made similar theoretical studies for oxygen on quartz[26] or β-cristobalite.[27,28] Up to now, the published theoretical γ_O coefficients are directly estimated from calculated reaction probabilities of ER and Langmuir-Hinshelwood (LH) reactions. A very recent study on the O/O_2-β-quartz surface catalysis based on molecular dynamics simulations using a ReaxFF potential,[29] presents γ_O coefficients for O or O/O_2 gases at very high pressures (10–100 atm) in the temperature range of 500–2000 K, which are larger than most experimental values.

In the present work, we carry out new QCT thermal studies for the principal elementary processes (*i.e.*, ER, O and O_2 reaction dynamics) and we propose a microkinetic model for thermal O/O_2 mixtures reacting over a β-cristobalite (001) surface. All kinetic parameters are derived mainly from QCT data; the corresponding γ_O and β_O coefficients for different temperatures and partial/total pressures are predicted. To our knowledge it is one of the few macroscopic models for this kind of systems, which only use theoretical data, in a similar way as we did in a previous work for O/O_2 over graphite (0001).[30]

2. Quasiclassical trajectory studies

We have performed a QCT dynamics study[31] of atomic and molecular oxygen colliding with a clean β-cristobalite (001) surface. We have also studied the O collisions with an O-precovered β-cristobalite (001) surface to investigate the ER reaction. These processes were previously studied at several state-specific conditions (*e.g.*, initial collision energy (E_{col}), internal $O_2(v,j)$ states,...) and only in few thermal (or quasithermal) conditions.[22–25] Here we increase the temperature range (300–1600 K) and improve the statistics of the calculated reaction probabilities. The present study makes use of the previous developed PES for the global O_2/β-cristobalite system,[23] based on DFT data interpolated *via* by the corrugation reduction procedure.[32] In an earlier work[21] we extensively showed that spin-polarized DFT-GGA-PW91 calculations seemed to be accurate enough to describe not only the bulk properties of silica but also the interaction of oxygen and nitrogen over several β-cristobalite faces. The interpolated PES was based on a dense grid of DFT-GGA-PW91 points calculated for several O and O–O configurations over the 1×1 surface unit cell,[23] taking the lowest energy state (essentially singlet at short surface distances and triplet for longer ones). An empirical silica slab was also used to introduce the slab motion. Therefore, the present multidimensional PES allows both the oxygen and β-cristobalite movements. A wide description of this adiabatic PES (*e.g.*, expressions, parameters, plots,...) are reported in previous papers.[22,23] We have used the same PES (available upon request) in the present study although we have added a small correction in two subroutines to make sure that the Cartesian gradients were fully periodic for atom/slab calculations with cells larger than the 1 × 1 one. Previous studies should not be affected by this fact as we used also the 1 × 1 unit cell, mainly for normal incidence calculations.

For O collisions with the clean surface we keep the second O atom at a large enough distance to the surface to avoid any undesirable interaction.

The QCT description has been widely presented elsewhere.[22,23] Briefly, the β-cristobalite slab used is formed by 104 atoms distributed into 9-layers for a 2 × 2 surface unit cell with a lattice parameter of 7.348 Å. The slab temperature (T_S) was controlled by means of a generalized Langevin equation approach.[31,33] The initial position of the incoming atomic or molecular oxygen was sampled over an 1 × 1 surface unit cell, with an initial distance higher than 6 Å to avoid s ignificant surface interaction. For the ER study the adsorbed

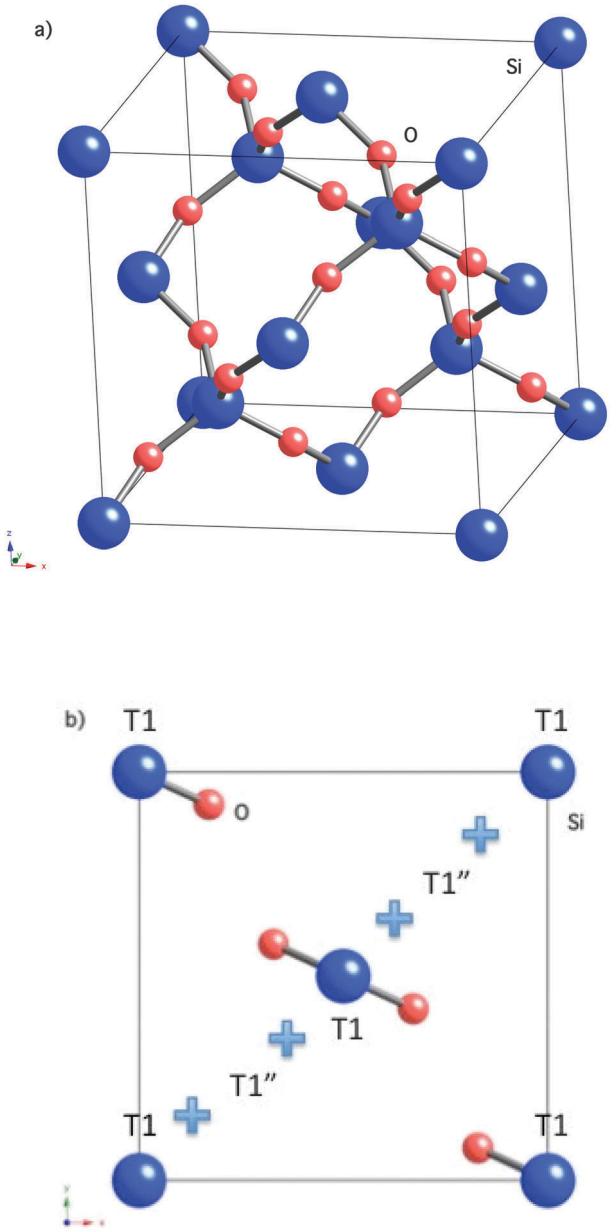

Fig. 1 Fdd2-β-cristobalite unit cell formed by Si (large spheres) and O (small spheres) atoms: (a) 3D unit cubic cell and (b) top view of the (001) face showing the two first layers and the T1 (Si) and T1′′ (crosses) sites.

O atom (O_{ad}) was located over the central Si atom of the first layer (T1/T1′′ sites, Fig. 1) at an initial z distance of around 1.5 Å, being also thermalized together with the slab. Since the experimental measurements of γ_O on β-cristobalite[8] correspond approximately to a flux of air colliding normally to the surface, we have restricted our simulation to normal incidence ($\theta_v = 0°$) for all atomic and molecular collisions. Thus, as we are interested in quasithermal conditions (*i.e.*, $T = T_{O_{(g)}} = T_{O_{2(g)}} = T_S$, θ_v), the remaining conditions (*i.e.*, initial O or O_2 centre of mass position, azimuthal velocity ϕ_v angle, molecular ϕ and θ angles,...) were randomly sampled and (E_i, v, j) were also sampled from a Boltzmann distribution at each selected temperature (T). Hamilton's equations were integrated by means of a modified Beeman algorithm with a fixed step of 1×10^{-4} ps, which permits an energy conservation of 10^{-4}–10^{-5} eV in absence of the thermal bath.

Batches of 5000–15 000 trajectories were integrated at each temperature to ensure a reasonable good statistics for the reaction probabilities of the main channels. Different processes could be observed: atomic and molecular reflection, atomic and molecular sticking (adsorption + absorption), $O_{2(ad)}$ formation and $O_{2(g)}$ formation (*i.e.*, ER reaction). Classification criteria for these events were broadly discussed in earlier works.[22,23] These were based mainly on the analysis of Z_O, $Z_{O'}$, Z_{CM} (molecular centre of mass Z coordinate) and r (O–O distance) variables, and the corresponding z velocity components of the atoms or the molecule (v_{zCM}) after a minimum collision time (*e.g.*, $t = 2$ ps). Thus, molecular oxygen (gas) was formed by the ER reaction when Z_{CM} was much larger than 6 Å, the r distance was shorter than the double of the equilibrium distance (*i.e.*, $r < 2.5$ Å) and $v_{zCM} > 0$, whereas $O_{2(ad)}$ was classified when $Z_{CM} < 3.0$ Å with $r < 2.5$ Å. For this latter case, the integration was really finished if after some extra steps (*e.g.*, 5–10) the classification was preserved. This criterion was especially useful for channels involving finally adsorbed/absorbed species. Nevertheless, some trajectories were ended up at shorter collision times ($t < 2$ ps) due to some PES limitations for extrapolation (*e.g.*, the PES is not defined for $Z_{CM} < 0$, $Z_O < -1.0$ A or $r < 0.5$ Å), although we think that the final thermal probabilities are even pretty well converged and accurate enough for rate constant calculations.

Fig. 2 summarizes the reaction probabilities for quasi-thermal conditions from 300 to 1600 K. Fig. 2a presents the O collisions over a clean surface, observing a very strong sticking, which decreases with the temperature raise. A much lower sticking is observed in Fig. 2b for O_2 collisions over a clean surface. These behaviours were previously explained due to the favourable adsorption of both species (mostly for O) over several sites of the Si-terminated β-cristobalite surface, especially on top (T1 site) or very close (T1′ and T1′′ sites) to Si atoms[23] (see Fig. 1). Molecular dissociative adsorption is not observed in this temperature range in agreement with previous QCT studies[24,25] that predict that this process is only open at higher collision energies (*e.g.*, $E_i > 1$ eV). Fig. 2c and d show the reaction probabilities for O collisions with an O-precovered surface (O on T1/T1′′ site, which means an atomic coverage $\theta_O = 0.25$). The atomic sticking decreases in comparison with the clean surface probabilities as new processes such as O_2 formation appear. In fact, we distinguish between the formation of the $O_{2(g)}$ *via* the ER reaction and the production of molecular oxygen that is strongly retained on the surface ($O_{2(ad)}$). This second reaction channel is much more probable than the first one, which is shown in a semilogarithmic scale in Fig. 2d. This trend was also observed in similar studies of atomic oxygen recombination over quartz[26] and in previous molecular dynamic simulations for O/O_2 over β-quartz.[29] In this latter study, $O_{2(ad)}$ formation was established if adsorption was longer than 5 ps, although simulations at very long times (*i.e.*, 1.5 ns) showed important O_2 desorption, which increased the final ER probabilities and

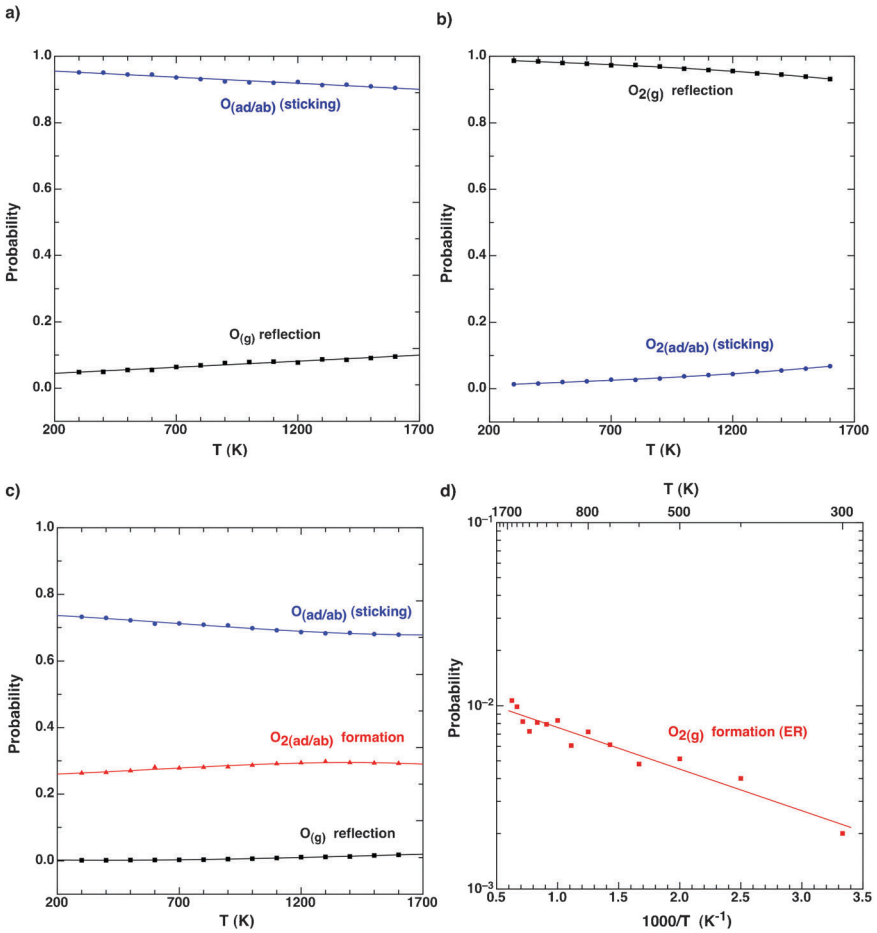

Fig. 2 QCT reaction probabilities for normal incidence at several temperatures (300–1600 K): (a) O over a clean surface, (b) O_2 over a clean surface, (c) and (d) O over an O-precovered surface. Lines show analytical fittings.

hence their γ coefficients, although possibly this should be classified instead as molecular desorption. The comparison of the present probabilities (Fig. 2c and d) with our previous ones[23] show small differences (*i.e.*, lower O_2 sticking and consequently larger O sticking for O collisions over an O-precovered surface, because the sum of probabilities is the unity) mainly originated by the introduction in our QCT code of a different classification of $O_{2(ad)}$ events (*e.g.*, $Z_{CM} < 3.0$ instead of 1.9 Å, which was used in the previous study[23]). The use of longer integration times in our trajectories (*i.e.*, $t > 2.5$ ps) could also increase a bit the final O_2 desorption although the mentioned PES limitations (*i.e.*, energy extrapolation at very short O or O_2 distances to the surface) avoid to describe more accurately such process.

3. Microkinetic modelling of O/O_2 mixtures reacting over β-cristobalite

3.1 Surface processes

We propose a first microkinetic model to ascertain the global effect of the main heterogeneous processes involving different O/O_2 mixtures over a β-cristobalite (001) surface at quasi-thermal conditions. Ten surface elementary processes are included, where i will be used for the direct processes and $-i$ for their reverse ones ($i = 1,\ldots,5$). These are:
chemisorption (k_1) and desorption (k_{-1}) of oxygen atoms,

$$O_{(g)} + s \rightleftarrows O_{(ad)} \quad (1)$$

molecular nondissociative adsorption (k_2) and molecular desorption (k_{-2}),

$$O_{2(g)} + 2s \rightleftarrows O_{2(ad)} \quad (2)$$

$O_{2(ad)}$ formation by atomic recombination (k_3) and molecular dissociative desorption (k_{-3}),

$$O_{(g)} + O_{(ad)} + s \rightleftarrows O_{2(ad)} \quad (3)$$

Eley-Rideal reaction (k_4) and molecular dissociative adsorption (k_{-4}),

$$O_{(g)} + O_{(ad)} \rightleftarrows O_{2(g)} + s \quad (4)$$

and Langmuir-Hinshelwood reaction (k_5) and molecular dissociative adsorption (k_{-5}),

$$O_{(ad)} + O_{(ad)} \rightleftarrows O_{2(g)} + 2s \quad (5)$$

where s indicates a free site on the surface. DFT studies show that molecular oxygen is adsorbed in parallel over a Si atom,

using two free adjacent sites of the four available in each (1 × 1) unit cell.[23] The O_2 dissociation can produce several final products (*e.g.*, $O_{(ad)} + O_{(ad)}$, $O_{(g)} + O_{(ad)}$,...). Adsorbed (ad) or absorbed (ab) species are indicated hereafter using only the *ad* subscript, as they are not distinguished within this model. Processes are labelled as direct and reverse ones for notation compactness (*i.e.*, k_i and k_{-i}).

3.2 Thermal rate constants

We have calculated the thermal rate constants for the elementary processes (1), (2), (3) and (4) from the corresponding thermal QCT reaction probabilities ($P_i(T)$) reported in section 2 (Fig. 2) by using conveniently the following standard expressions,[6,12]

$$k_i(T) = P_i(T)\sqrt{\frac{k_B T}{2\pi m_l}}\frac{1}{[s]_0}, \quad i = 1,4 \ (m^3\ s^{-1}) \tag{6}$$

$$k_i(T) = P_i(T)\sqrt{\frac{k_B T}{2\pi m_l}}\frac{1}{[s]_0^2}, \quad i = 2,3 \ (m^5\ s^{-1}) \tag{7}$$

where k_B is the Boltzmann constant, T is the temperature, m_l is the atomic mass (molecular mass for k_2) and $[s]_0$ is the initial surface density of free sites (*i.e.*, 4 sites per unit cell or 7.41×10^{18} sites m^{-2} for a β-cristobalite (001) surface). The i values in the eqn (6) and (7) show the elementary processes for which these rate constants are calculated.

We have used fittings of the QCT probabilities by using some polynomials for (1), (2) or (4) processes or an Arrhenius expression for ER reaction (3), which are also plotted in Fig. 2. As the LH reaction was not studied by the QCT method, we have estimated its rate constant from the following equation,[6,12]

$$k_5(T) = \frac{1}{\Delta}\sqrt{\frac{\pi k_B T}{2m_O}}\frac{1}{[s]_0}e^{-\Delta E_5^{0\neq}/k_B T}, \quad (m^2\ s^{-1}) \tag{8}$$

where Δ is the mean distance between active sites, the square root term is the mean velocity of O reacting adatoms, assuming a two-dimensional gas and $\Delta E_5^{0\neq}$ is the LH energy barrier including zero point energy, derived from our PES data (*i.e.*, $\Delta E_5^{0\neq} \approx \Delta E_5^0 = 3.29$ eV). The rate constants for reverse processes (k_{-i}) were obtained by means of the principle of detailed balance, using the DFT reaction *exo*- or endothermicities of each process (ΔE_i^0, including zero point energies). We have not introduced spin statistical factors into the rate constants. This assumption could be acceptable as we use the same adiabatic PES for all O_2/β-cristobalite processes and because these factors should produce only small and similar changes into the calculate rate constants.

Fig. 3 shows the calculated QCT rate constants within the 400–2000 K range of temperature. The great differences in these rate constants will have an important influence on the global recombination kinetics of the system. It is for instance expected that LH reaction contributes much less than ER reaction to the global recombination within this model.

The rate constants are finally fitted by using an Arrhenius formula within the 700–1700 K range, whose parameters (A_i, $E_{a,i}$) are indicated in Table 1 together with ΔE_i^0 values. This more restricted temperature range is selected to obtain better Arrhenius parameters to be used for the following γ_O and β_O calculations; the initial T interval is too wide (400–2000) so that significant curvature is observed at lower temperatures.

3.3 Surface coverage and γ_O recombination coefficient

The time evolution of the surface concentration of both atomic and molecular adsorbed species resulting from the microkinetic model is given by the solution of the coupled equations

$$\begin{aligned}\frac{d[O_{(ad)}]}{dt} &= k_1[O][s] - k_{-1}[O_{(ad)}] - k_3\frac{1}{3}[O][O_{(ad)}][s] \\ &\quad + k_{-3}[O_{2(ad)}] - k_4[O][O_{(ad)}] + k_{-4}[O_2][s] \\ &\quad - 2k_5[O_{(ad)}]^2 + k_{-5}\frac{1}{3}[O_2][s]^2\end{aligned} \tag{9}$$

and

$$\begin{aligned}\frac{d[O_{2(ad)}]}{dt} &= k_2\frac{1}{3}[O_2][s]^2 - k_{-2}[O_{2(ad)}] \\ &\quad + k_3\frac{1}{3}[O][O_{(ad)}][s] - k_{-3}[O_{2(ad)}]\end{aligned} \tag{10}$$

where as each $O_{2(ad)}$ uses two sites, the density of free adsorption sites at any time will be

$$[s] = [s]_0 - [O_{(ad)}] - 2[O_{2(ad)}] \tag{11}$$

Fig. 1 shows the available sites over the unit cell of β-cristobalite (001) surface. The incoming O atom approaches preferentially the surface over Si atoms (T1 sites) but at closer distances the adatom can be tilted over the more stable T1″ sites as was shown in previous studies.[22] Thus, every Si can adsorb two O atoms using its two dangling bonds. The factor 1/3 takes into account that only the nearest neighbours (*i.e.*, two O on the same Si) will be effective for several reactions (*e.g.*, two adjacent sites inside the unit cell, which means one of the three pairs of sites, are necessary for reaction (2)). In fact, this small correction introduces some correlation between the locations of the reactants on the surface that a phenomenological kinetics approach does not take into account as compared with more accurate kinetic Monte Carlo simulations.[34]

The numerical integration of these differential equations (eqn (9) and (10)) for a constant flux of an O/O_2 mixture (*i.e.*, constant P_O and P_{O_2}) impinging against the surface at a given temperature allows monitoring the evolution of atomic (θ_O) and molecular (θ_{O_2}) coverages up to final steady-state (ss) as shown in Fig. 4 at 900 and 1500 K for $P_O = 91$ Pa and $P_{O_2} = 9$ Pa. These partial pressures are close to the experimental ones for highly dissociated air plasma (*ca.* 70–80%)[8,35] at total pressure of 200 Pa over β-cristobalite. Two different trends are observed: (a) a final molecular coverage at temperatures lower than 1000 K, which occurs at much longer times and (b) a final predominant and very high atomic coverage at high temperatures. These overall behaviours are observed for several mixtures; however, the formation of $O_{2(ad)}$ by the competitive processes (2) and (3), which have similar rate constants (Fig. 3), increases mainly with the raise of P_{O_2} and P_O, respectively, hence alternating their

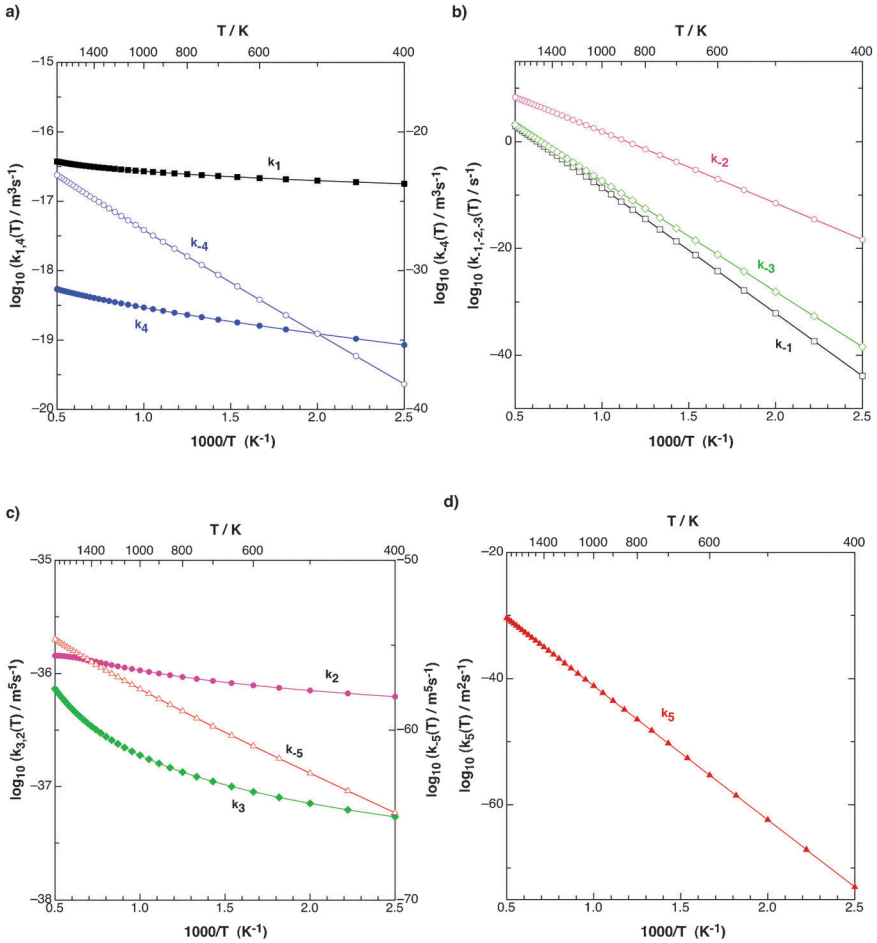

Fig. 3 Calculated thermal rate constants (400–2000 K) for the different heterogeneous processes involved in the proposed microkinetic model, based on QCT data. Only rate constants with the same units can be easily compared. Points are connected with a line to guide the view.

influence for different initial mixtures. For pure O mostly atomic coverage is observed.

$$\gamma_O = \frac{k_1[O][s]_{ss} - k_{-1}[O_{(ad)}]_{ss} + k_3\frac{1}{3}[O][O_{(ad)}]_{ss}[s]_{ss} - k_{-3}[O_{2(ad)}]_{ss} + k_4[O][O_{(ad)}]_{ss} - k_{-4}[O_2][s]_{ss}}{Z_O} \quad (12)$$

The difference between both behaviours are mainly originated from the temperature dependence of both molecular desorption processes (−2) and (−3). At very high temperatures their rate constants (k_{-2}, k_{-3}) are very large (being $k_{-2} \gg k_{-3}$) and only a final atomic adsorption is observed (*e.g.*, $\theta_O = 0.99$ at 1500 K, Fig. 4b), being negligible the final $O_{2(ad)}$ formation by (2) or (3) processes. At lower temperatures atomic oxygen is initially adsorbed until a suitable atomic coverage (maximum in Fig. 4a), when reaction (3) starts to produce $O_{2(ad)}$, which is not desorbed enough because both k_{-2} and k_{-3} (also with $k_{-2} \gg k_{-3}$) are now much lower (*e.g.*, $\theta_O = 0.11$ at 900 K, Fig. 4a). The calculated atomic and molecular coverages are much larger that the ones observed for graphite (0001) ($\theta_O < 10^{-3}$ and $\theta_{O_2} \approx 0$),[30] which can be justified by the very strong atomic and molecular chemisorptions on β-cristobalite.

We have also calculated the atomic oxygen recombination coefficient γ_O as the ratio of the total flux of recombining oxygen atoms ($O_{(g)}$ consumption and formation) to the initial flux of impinging oxygen atoms (Z_O) over the surface once achieved the steady-state concentrations, using the following equation,

Z_O, which is the number of O collisions over a surface per unit area and unit time, is given by the standard Hertz-Knudsen relation,[36]

$$Z_O = [O]\sqrt{\frac{k_B T}{2\pi m_O}} \quad (13)$$

for a constant and normal flux of O/O_2 (*i.e.*, $[O] = [O]_0$ and $[O_2] = [O_2]_0$). We have checked that the γ_O coefficient derived from O_2 balance[16,36] led to the same values than the ones from eqn (12) at the final steady-state (or quasisteady-state). At lower temperatures, the surface suffers a passivation ($\gamma_O \approx 0$) due to the high O_2 coverage, which prevents any atomic recombination. Therefore, in this case we have estimated γ_O coefficient at the quasisteady-state reached at shorter times, which is comparable with experimental measurements on β-cristobalite.[8] Fig. 5 shows γ_O dependency against the inverse of the temperature, splitting this among the three main contributions: (1), (3) and (4) processes. We observe that γ_O

Table 1 Arrhenius parameters derived from the calculated thermal rate constants using analytical $P_i(T)$ QCT probabilities within 700–1700 K. ΔE_i^0 are the *exo*- or endothermicities energies. Q_i energies and F_i fluxes are used later for β calculations

Reaction process	A[a]	$E_{a,i}$ (eV)	ΔE_i^0 (eV)[b]	Q_i[c]	F_i (m^{-2} s^{-1})[d]
1	4.404×10^{-17}	0.0407	−4.65	$E_{a,-1} - E_{a,1}$	k_1[O][s]
−1	5.018×10^{-14}	4.63	4.65	$-E_{a,-1}$	k_{-1}[$O_{(ad)}$]
2	1.980×10^{-36}	0.0518	−2.72	$\frac{1}{2}(E_{a,-2} - E_{a,2})$	$(1/3)k_2$[O][s]^2
−2	9.730×10^{-14}	2.60	2.72	$\frac{1}{2}(-E_{a,-2})$	k_{-2}[$O_{2(ad)}$]
3	1.285×10^{-36}	0.158	−4.07	$E_{a,-3} - E_{a,3}$	$(1/3)k_3$[O][$O_{(ad)}$][s]
−3	3.492×10^{-13}	4.14	4.07	$-E_{a,-3}$	k_{-3}[$O_{2(ad)}$]
4	8.686×10^{-19}	0.0914	−1.36	$-E_{a,4}$	k_4[O][$O_{(ad)}$]
−4	4.802×10^{-20}	1.53	1.36	$-E_{a,-4}$	k_{-4}[O_2][s]
5	1.663×10^{-20}	4.24	3.29	$\frac{1}{2}(-E_{a,5})$	$2k_5$[$O_{(ad)}$]^2
−5	8.069×10^{-53}	1.08	−3.29	$\frac{1}{2}(-E_{a,-5})$	$(1/3)k_{-5}$[O_2][s]^2

[a] Units (s^{-1}, m^3 s^{-1}, m^2 s^{-1} and m^5 s^{-1}) are as for the rate constants (see Fig. 1). [b] Values derived from the interpolated O_2/β-cristobalite PES, including zero point energies. Atomic adsorption assumed on T1 site. [c] Energies by O atom required (<0) or released (>0) to the surface for each *i* process. [d] Partial atomic or molecular fluxes for each reaction process.

is almost independent on the initial mixture composition, as we have verified for some initial conditions (*e.g.*, P_O/P_{O_2} = 0.1, 1, 10 at several total pressures lower than 5000 Pa). Atomic oxygen recombination is almost insensitive to the presence of molecular oxygen in the initial flux because of the very low rate constants of the processes (2), (−4) and (−5) involving O_2 (see Fig. 3), leading to negligible molecular dissociative or nondissociative adsorptions. However, at very large pressures these processes could become more important (*i.e.*, through the concentration effect in eqn (12)) as it was shown for O recombination over β-quartz at 100 atm,[29] where for O/O_2 mixtures with partial pressures of 50 atm the γ_O coefficient decreased with respect to pure O at 100 atm.

Small recombination coefficients are observed ($0.01 < \gamma_O < 0.02$) in the 700–1700 K range, which are essentially originated from atomic adsorption and ER reaction with a similar proportion. No LH contribution is observed at all. In spite of the reaction (3) competes with ER reaction (4) with much higher reaction probabilities (Fig. 2c and d), its lower rate constants (*i.e.*, $k_3 < k_4$; see Fig. 3a and c) together with the small amount of free surface sites (see $[s]_{ss}$ in Fig. 4), can justify its negligible contribution to γ_O.

These two contributions in γ_O are in agreement with previous assumptions made in similar kinetic models.[5,37] At very large pressures the LH reaction seems to gain importance for β-quartz,[29] leading to larger γ_O values ($0.01 \leq \gamma_O \leq 0.35$).

Fig. 6 compares the calculated γ_O values with recent molecular dynamics calculations on O/O_2 over β-quartz[29] along with experimental measurements on several silica surfaces.[8,38–40] The calculated coefficients increase with T following an

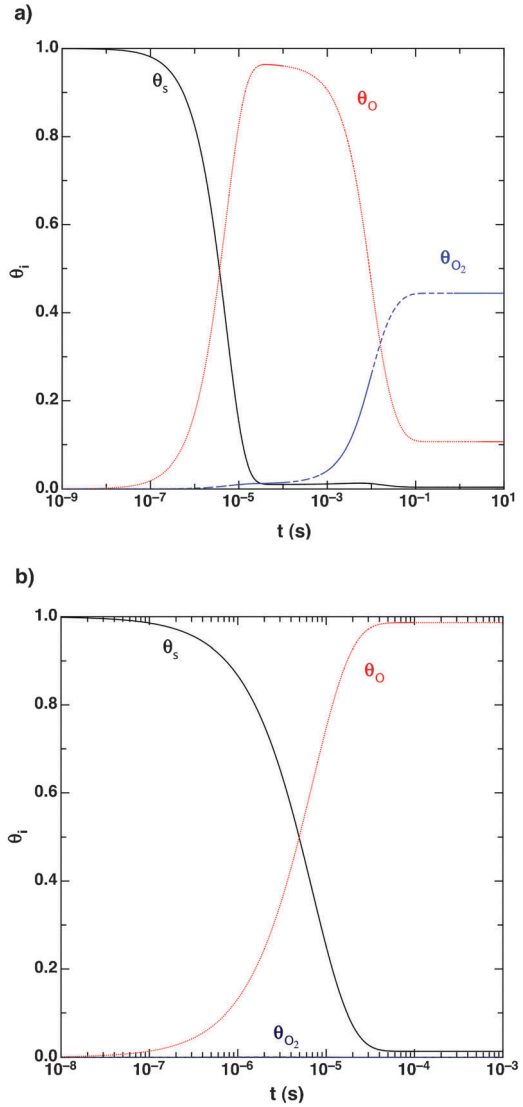

Fig. 4 Free sites fraction, and atomic and molecular surface coverage evolutions for an O/O_2 mixture (91, 9 Pa) at (a) 900 K and (b) 1500 K.

exponential trend in agreement with the scattered experimental data. The dispersion in the experimental data may be due to several factors such as composition and structure of the silica surface (*i.e.*, amorphous silica, several crystalline polymorphs,...), surface roughness,[4,38] gas composition (*e.g.*, air, pure O, O/O_2 mixtures,...) or the experimental method used. The present calculated γ_O coefficients correspond to a perfect β-cristobalite (001) surface. The introduction of defects in our surface (*e.g.*, corners, steps, O vacants,...) would modify somewhat the reactivity and consequently the calculated γ_O coefficient. In fact, the experimental measurements used a β-cristobalite surface coating[8] obtained by oxidation of sintered SiC samples at different temperatures, with possibly a polycrystalline nature, which could justify the slightly higher experimental reactivity.

In a previous work[23] we directly compared the experimental γ_O values with QCT ER reaction probabilities, obtaining similar values although with a slope closer to the experimental one than that of the present work. The seemingly better

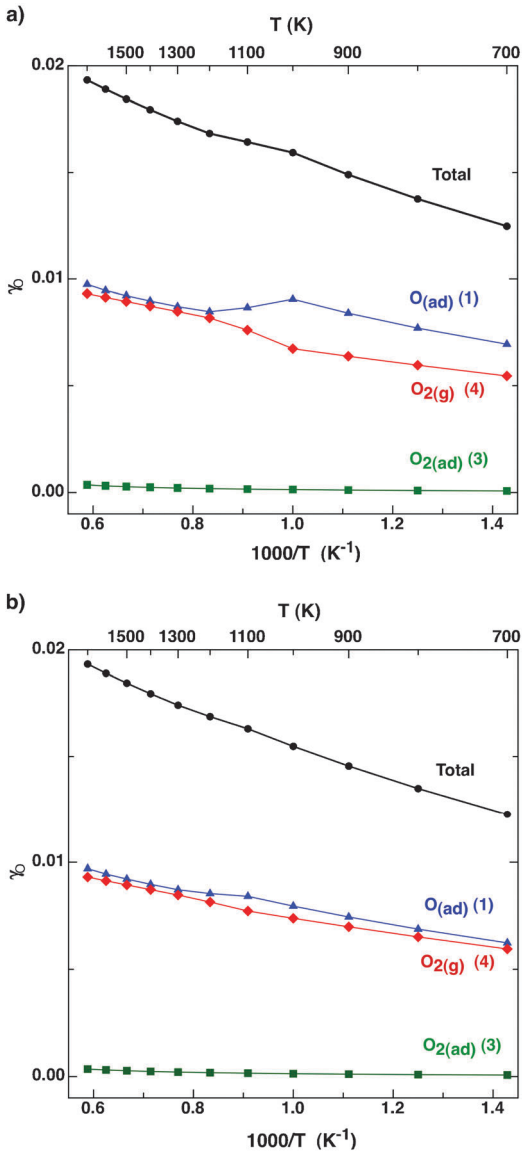

Fig. 5 Calculated $\gamma_O(T)$ coefficients *versus* the reciprocal of the temperature, showing their main process contributions: (a) P_O = P_{O_2} = 50 Pa, (b) P_O = 100 Pa, P_{O_2} = 0.

previous results could be fortuitous because another processes (*e.g.*, specially the atomic adsorption) should be included in a more reliable calculation of this coefficient. On the other hand, as the calculated γ_O coefficients are based on QCT reaction probabilities, some improvements on those could increase slightly the γ_O values. Thus, the inclusion of physisorbed O atoms (not only chemisorbed on T1/T1″ sites) in the ER study would probably increase the O_2 formation. Moreover, the integration at longer times (*e.g.*, 2.5–5 ps) for reaction (3), which produces adsorbed O_2, could increase the molecular desorption with following final augment of the ER contribution. For instance, simulations for β-quartz[29] were ran at least for $t < 5$ ps, showing also a significantly increasing of γ_O but possibly at too long times (*i.e.*, 1.5 ns).

Finally, although microkinetic models are commonly used to simulate the heterogeneous chemical kinetics of dissociated airflows impinging different types of surfaces[16,36] with good

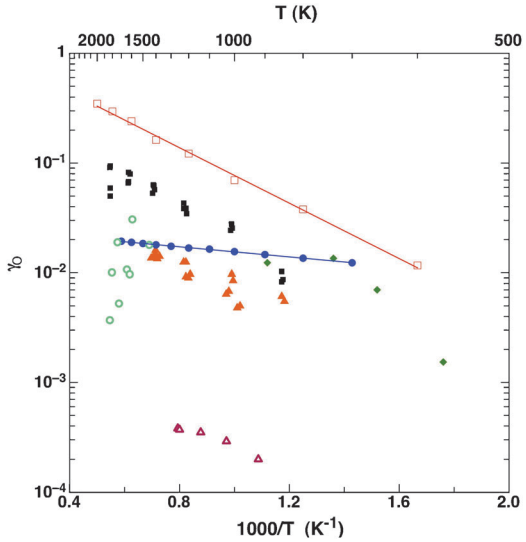

Fig. 6 Calculated and experimental $\gamma_O(T)$ coefficients *versus* the reciprocal of the temperature for several silica materials. The solid lines show an Arrhenius fitting of the calculated data. Calculated γ_O: this work for O/O_2 (P_O = 91 Pa, P_{O_2} = 9 Pa) on β-cristobalite (filled circles); ReaxFF Molecular Dynamics calculations for pure O at 1 × 10^6 Pa on β-quartz (empty squares).[29] Experimental γ_O: air on β-cristobalite (filled squares) and quartz (filled triangles) at 200 Pa;[8] pure O on fused quartz at 27 Pa (empty triangles);[38] O on silica (vitreosil) at P_O = 1500–1600 Pa (filled diamonds);[39] $\gamma_{O'}$ for O on RCG at P_O = 133–824 Pa (empty circles).[40]

agreement in comparison to available experimental data (*e.g.*, total heat flux to the surface, γ coefficients,...), more developed Monte Carlo simulations (*e.g.*, N over silica,[41] H over graphite[42]) could also be needed to provide a deeper microscopic understanding of these processes.

3.4 β_O chemical energy accommodation coefficients

Following a similar approach as for the calculation of γ coefficient, we can calculate the β coefficient once achieved the final steady- or quasisteady-state from the ratio of the total chemical energy that can be transferred to the surface to the energy that would be released if all consumed O atoms gave place to O_2(g), using the expression

$$\beta = \frac{\sum_{i=-5, i\neq 0}^{+5} F_i \cdot Q_i}{Z_O \cdot \gamma \cdot (D_{O_2}/2)} \qquad (14)$$

where D_{O_2} is the O_2 dissociation energy, F_i represents the atomic or molecular fluxes at the steady-state (shown in Table 1) and Q_i are the energies per O atom required or released in each process, which are derived from the expressions and activation energies (Table 1). We assumed that adsorbed species (*e.g.*, process (1)) release all of their available energy to the surface and that gas products (*e.g.*, process (4)) will escape with all of their available energy (*i.e.*, assuming a very short interaction with the surface), which would give a minimum β. This latter point is supported by previous QCT study of the ER reaction on β-cristobalite,[23] which showed that formed O_2 molecules become translationally and internally excited, taking rather some energy from the surface.

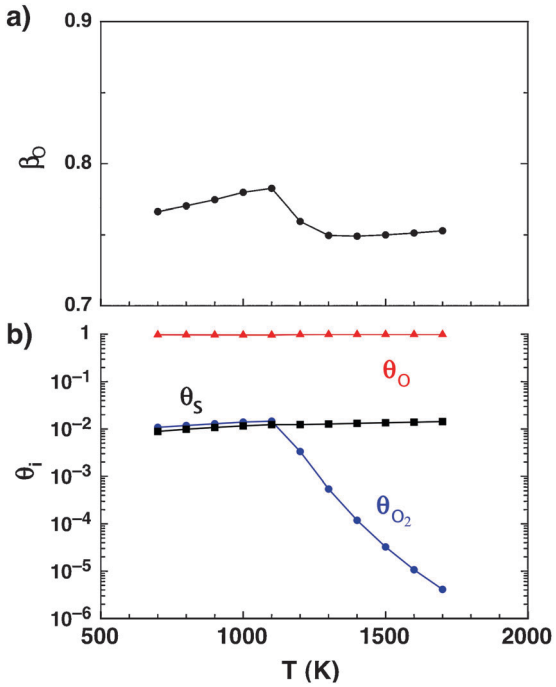

Fig. 7 Calculated $\beta_O(T)$ coefficients and surface coverage for an O/O_2 mixture (91, 9 Pa) over on β-cristobalite at several temperatures.

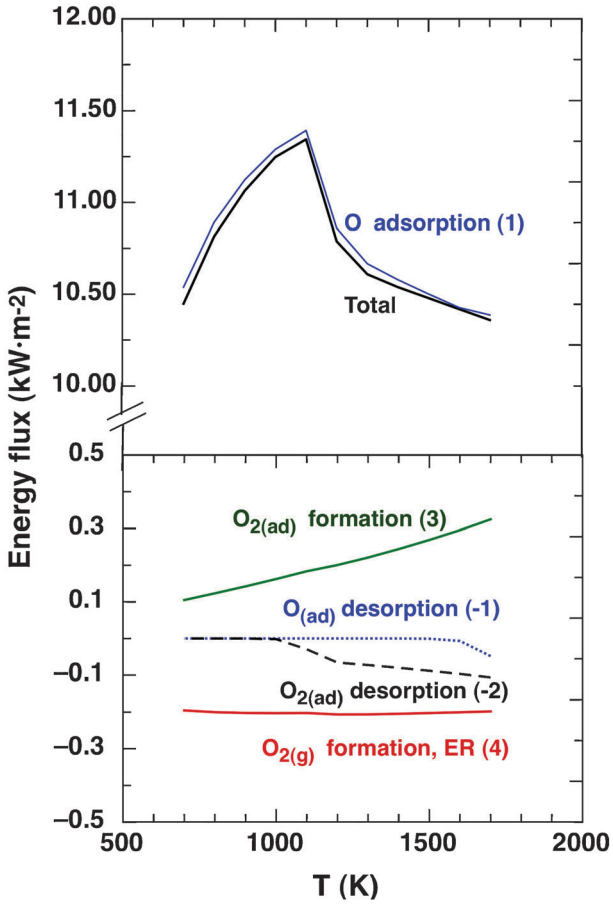

Fig. 8 Calculated total and partial ($F_i \cdot Q_i$) energy fluxes transferred with the β-cristobalite surface for an O/O_2 mixture (91, 9 Pa) at several temperatures. The main contributions of the different processes are also shown. Be careful because the lower panel uses a much more amplified Y-axes (1 kW m^{-2}).

Similar expressions were used in earlier studies[5] to estimate this β coefficient under several assumptions. This calculation should be considered as a first approximation to this coefficient (β_{min}) as there is not a unique choice of Q_i energies. Detailed dynamics studies on each elementary process, determining their energy fluxes with the solid, could afford a much accurate β calculation. Fig. 7a presents β_O as a function of temperature for the same conditions as for Fig. 6, showing a value within the 0.75–0.80 range. There is only a very slight dependency with the temperature with a small maximum around 1100 K, which arises from the small decrease in molecular coverage (see Fig. 7b) due to the desorption process (−2) becomes more important than the O_2 formation by process (3) for $T \geq 1100$ K, being in these conditions β proportional to $k_1 \cdot [s]/\gamma \cdot T^{1/2}$. A similar shape with almost constant β values were found for instance for N recombination over palladium and rhodium.[5] We have also calculated β_O for several initial O/O_2 mixtures with similar results; only for $P_O = P_{O_2} = 50$ Pa the maximum achieved a larger value (*i.e.*, $\beta_O = 0.85$ at 1000 K). The values obtained show that the common assumption that $\beta_O = 1$ and hence $\gamma_{O'} = \gamma_O$ is not justified at all for O recombination over β-cristobalite. An analysis of the main contributions to β_O is shown in Fig. 8, which displays the total and the partial energy fluxes originated by the main processes. Clearly, the atomic adsorption process is largely the one producing almost the total energy released to the surface.

Up to our knowledge there is only a communication[43] about some direct measurements of β_O and catalytic recombination fluxes on β-cristobalite, which reports a strong decrease of this coefficient in the interval 966–1770 K at 200 Pa ($0.69 < \beta_O < 0.12$), but with a surprising almost constant energy flux (*e.g.*, 35 ± 5 kW m^{-2} for the lowest and highest β_O values) in this temperature range. The same authors have presented the effective catalycity ($\gamma_{O'} = \gamma_O \cdot \beta_O$), which decreases slightly as temperature augments[7] contrary to the common increase of $\gamma_{O'}$ observed for several silica materials (*e.g.*, RCG, SiO_2 + B_2O_3,...[7]). The present calculations show nearly constant β_O coefficients and energy fluxes, showing however lower values (10.4–11.3 kW m^{-2} for $P_O = 91$ Pa, $P_{O_2} = 9$ Pa) and a different behaviour particularly respect to β_O. The experimental recombination fluxes increase for more catalytic materials ($SiC \approx SiC + SiO_2 \leq AlN \leq Al_2O_3$);[44] thus sintered SiC shows a nearly constant value (25 or 35 kW m^{-2} for air at 200 or 2000 Pa, respectively) while pure alumina reaches 184 kW m^{-2} at 1400 K, decreasing to 93 kW m^{-2} at 1800 K for 2000 Pa.[44] The experimental increase of this flux as pressure rises (*e.g.*, from 200 to 2000 Pa) could also indicate the necessity of a better understanding of the experimental conditions in order to facilitate a more reliable comparison with our calculations. For instance, we observe also this increase for higher oxygen pressures (*e.g.*, a mean value of 23.5 kW m^{-2} for $P = P_O = 200$ Pa). Moreover, new measurements of β_O for pure oxygen mixtures would be necessary to see if the results for air are reliable enough and to compare more properly with the present calculations.

4. Summary and conclusions

In this work we present a theoretical study of a gas mixture of atomic and molecular oxygen reacting over a β-cristobalite (001) surface, which is relevant for the simulation and the understanding of the aerodynamic heating produced during the reentry of spacecraft into Earth's atmosphere.

We use a previous multidimensional potential energy surface based on DFT data to determine thermal rate constants for atomic or molecular oxygen colliding with a clean surface and for atomic oxygen colliding with an O-precovered surface, by means of quasiclassical trajectories.

The present dynamical studies confirm earlier conclusions: atomic sticking over the clean surface is the predominant process but decreases for an O-precovered surface due to the appearance of two competitive processes that produce $O_{2(ad)}$ and $O_{2(g)}$. Moreover, molecular nondissociative sticking is also observed.

We propose a microkinetic model with ten heterogeneous processes to study this system for different O/O_2 mixtures and temperatures. Rate constants are derived from QCT data for direct processes or using the principle of detailed balance for reverse ones. The numerical integration of the corresponding differential equations allows determining the evolution of atomic and molecular surface coverage until the final steady-state. A large molecular coverage is observed at temperatures lower than 1000 K, which could produce surface passivation at long times, whereas a large atomic coverage at higher temperatures for O/O_2 mixtures is obtained.

We have calculated the atomic oxygen recombination coefficients, showing small values in the 700–1700 K range ($0.01 < \gamma_O < 0.02$) almost independent on the initial mixture composition, being the atomic adsorption and Eley-Rideal their main contributions. The calculated coefficients increase with the temperature following an Arrhenius equation in agreement with experimental data, with values close to the experimental ones.

An estimation of a minimum chemical energy accommodation coefficient has been also presented, obtaining an almost constant value ($0.75 < \beta_O < 0.80$) within 700–1700 K; therefore the common assumption that $\beta_O = 1$ and hence $\gamma_{O'} = \gamma_O$ seems inaccurate for O recombination over β-cristobalite. The atomic adsorption process is mostly the one producing almost the total energy released to the surface. Nevertheless, there are some divergences of the calculated β_O respect the only set of available experimental values for air over β-cristobalite, although the agreement is much better respect the total energy flux transferred to the surface. Additional measurements of γ_O and β_O for pure oxygen mixtures instead of for air and a better knowledge of the experimental conditions would be necessary to compare more correctly the present calculated coefficients.

Acknowledgements

This work was supported in part by the Spanish Ministry of Science and Innovation (Project CTQ2009-07647), by the Autonomous Government of Catalonia (Project 2009SGR1041) and by the European Commission research funding (Project FP7-SPACE-2009-242311). We also thank to Marianne Balat-Pichelin for the explanations about her experiments with air over β-cristobalite. The authors also thank to Prof. Ricardo Díez Muiño (Centro de Física de Materiales, Centro Mixto CSIC-UPV/EHU, San Sebastián, Spain) for fruitful discussions and to DIPC for financial support.

References

1 J. J. Bertin and R. M. Cummings, *Annu. Rev. Fluid Mech.*, 2006, **38**, 129–157.
2 M. Capitelli, R. Celiberto, F. Esposito and A. Laricchiuta, *Plasma Processes Polym.*, 2009, **6**, 279–294.
3 V. L. Kovalev and A. F. Kolesnikov, *Fluid Dyn.*, 2005, **40**, 669–693.
4 J. Thoemel, E. Cosson and O. Chazot, *Proceedings of the Sixth European Symposium on Aerothermodynamics for Space Vehicles*, Versailles, France, 2008, ESA **SP-659**, session 18, 1–14.
5 B. Halpern and D. E. Rosner, *J. Chem. Soc., Faraday Trans. 1*, 1978, **74**, 1883–1912.
6 T. Kurotaki, *AIAA*, 2000, **2366**, 1–7.
7 L. Bedra and M. Balat-Pichelin, *Aerosp. Sci. Technol.*, 2005, **8**, 318–328.
8 M. Balat-Pichelin, J. M. Badie, R. Berjoan and P. Boubert, *Chem. Phys.*, 2003, **291**, 181–194.
9 M. J. H. Balat-Pichelin, V. L. Kovalev, A. F. Kolesnikov and A. A. Krupnov, *Proceedings of the 24th International Symposium on Rarefied Gas Dynamics, AIP Conf. Proc.*, 2005, **762**, 1347–1352.
10 W. A. Seward and E. J. Jumper, *J. Thermophys. Heat Transfer*, 1991, **5**, 284–291.
11 E. J. Jumper and W. A. Seward, *J. Thermophys. Heat Transfer*, 1994, **8**, 460–465.
12 F. Nasuti, M. Barbato and C. Bruno, *J. Thermophys. Heat Transfer*, 1996, **10**, 131–136.
13 B. Gordiets, C. M. Ferreira, J. Nahorny, D. Pagnon, M. Touzeau and M. Vialle, *J. Phys. D: Appl. Phys.*, 1996, **29**, 1021–1031.
14 A. Daiss, H.-H. Frühauf and E. W. Messerschmid, *J. Thermophys. Heat Transfer*, 1997, **11**, 346–352.
15 G. Cartry, L. Magne and G. Cernogora, *J. Phys. D: Appl. Phys.*, 2000, **33**, 1303–1314.
16 V. Guerra, *IEEE Trans. Plasma Sci.*, 2007, **35**, 1397–1412.
17 M. Balat-Pichelin, V. L. Kovalev, A. F. Kolesnikov and A. A. Krupnov, *Fluid Dyn.*, 2008, **43**, 830–838.
18 M. Lino da Silva, V. Guerra and J. Loureiro, *Plasma Sources Sci. Technol.*, 2009, **18**, 034023.
19 I. Armenise, M. Capitelli, C. Gorse, M. Cacciatore and M. Rutigliano, *J. Spacecr. Rockets*, 2000, **37**, 318–323.
20 I. Armenise, M. Capitelli and C. Gorse, *J. Spacecr. Rockets*, 2001, **38**, 482–487.
21 C. Arasa, P. Gamallo and R. Sayós, *J. Phys. Chem. B*, 2005, **109**, 14954–14964.
22 C. Arasa, H. F. Busnengo, A. Salin and R. Sayós, *Surf. Sci.*, 2008, **602**, 975–985.
23 C. Arasa, H. F. Busnengo, A. Salin and R. Sayós, *Surf. Sci.*, 2009, **603**, 2742–2751.
24 R. Sayós, V. Morón, C. Arasa and H. F. Busnengo, *Proceedings of the Sixth European Symposium on Aerothermodynamics for Space Vehicles*, Versailles, France, 2008, ESA **SP-659**, session 28, 1–7.
25 V. Morón, C. Arasa, R. Sayós and H. F. Busnengo, *Proceedings of the 26th International Symposium on Rarefied Gas Dynamics, AIP Conf. Proc.*, 2008, **1084**, 682–687.
26 L. Bedra, M. Rutigliano, M. Balat-Pichelin and M. Cacciatore, *Langmuir*, 2006, **22**, 7208–7216.
27 M. Cacciatore, M. Rutigliano and G. D. Billing, *J. Thermophys. Heat Transfer*, 1999, **13**, 195–203.
28 M. Rutigliano, C. Zazza, N. Sanna, A. Pieretti, G. Mancini, V. Barone and M. Cacciatore, *J. Phys. Chem. A*, 2009, **113**, 15366–15375.
29 P. Norman and T. Schwartztentruber, *AIAA*, 2010, **4320**, 1–15.
30 V. Morón, P. Gamallo and R. Sayós, *Theor. Chem. Acc.*, 2011, **128**, 683–694.
31 G. D. Billing, *Dynamics of Molecule Surface Interactions*, John Wiley & Sons, New York, 2000 (ch. 5 and 6).

32 H. F. Busnengo, A. Salin and W. Dong, *J. Chem. Phys.*, 2000, **112**, 7641–7651.
33 J. C. Tully, *J. Chem. Phys.*, 1980, **73**, 1975–1985.
34 B. Temel, H. Meskine, K. Reuter, M. Scheffler and H. Metiu, *J. Chem. Phys.*, 2007, **126**, 204711-1–12.
35 M. Balat-Pichelin and A. Vesel, *Chem. Phys.*, 2006, **327**, 112–118.
36 M. Barbato, S. Reggiani, C. Bruno and J. Muylaert, *J. Thermophys. Heat Transfer*, 2000, **14**, 412–420.
37 S. Sepka, Y. Chen, J. Marschall and R. Copeland, *J. Thermophys. Heat Transfer*, 2000, **14**, 45–52.
38 Y. C. Kim and M. Boudart, *Langmuir*, 1991, **7**, 2999–3005.
39 J. C. Greaves and J. W. Linnett, *Trans. Faraday Soc.*, 1959, **55**, 1355–1361.
40 P. Kolodziej and D. A. Stewart, *AIAA.*, 1987, **87**, 1637–1647.
41 V. Guerra and J. Loureiro, *Plasma Sources Sci. Technol.*, 2004, **13**, 85–94.
42 H. M. Cuppen and L. Hornekaer, *J. Chem. Phys.*, 2008, **128**, 174707–1.
43 M. Balat-Pichelin, V. L. Kovalev, A. F. Kolesnikov and A. A. Krupnov, *AIP Conf. Proc.*, 2005, **762**, 1347–1352.
44 M. Balat, M. Czerniak and J. M. Badie, *Appl. Surf. Sci.*, 1997, **120**, 225–238.

